02 June 2004: pre-publication manuscript.
In press in: Psychiatry Research Neuroimaging

EEG microstate duration and syntax in acute, medication-naïve, first-episode schizophrenia: a multi-center study.

Dietrich Lehmann[a,*], Pascal L. Faber[a], Silvana Galderisi[b], Werner M. Herrmann[c,†], Toshihiko Kinoshita[d], Martha Koukkou[e], Armida Mucci[b], Roberto D. Pascual-Marqui[a], Naomi Saito[d], Jiri Wackermann[f], Georg Winterer[c], and Thomas Koenig[e]

[a]The KEY Institute for Brain-Mind Research, University Hospital of Psychiatry, Zurich, Switzerland

[b]Dept. of Psychiatry, University of Naples SUN, Italy

[c]Laboratory of Clinical Psychophysiology, Dept. of Psychiatry, University Hospital Benjamin Franklin, Free University of Berlin, Germany

[d]Dept. of Neuropsychiatry, Kansai Medical University, Osaka, Japan

[e]Dept. of Psychiatric Neurophysiology, University Hospital of Clinical Psychiatry, Bern, Switzerland

[f]Dept. of Empirical and Analytical Psychophysics, Institute for Frontier Areas of Psychology and Mental Health, Freiburg i.Br., Germany

Corresponding author:
*Prof. Dietrich Lehmann, M.D., The KEY Institute for Brain-Mind Research, University Hospital of Psychiatry, CH-8029 Zurich, Switzerland.
Tel: +41-1-388-4932;
FAX: +41-1-380-3043;
E-mail: dlehmann@key.unizh.ch.

With 3 Tables and 5 Figures (one of them in color).

Abstract
Introduction: In young, first-episode, productive, medication-naive schizophrenics, EEG microstates (building blocks of mentation) tend to be shortened. Koenig et al. (1999) suggested that shortening concerned specific microstate classes. Sequence rules (microstate concatenations, syntax) conceivably might also be affected.
Methods: In 27 patients of the above type and 27 controls, from three centers, multichannel resting EEG was analyzed into microstates using k-means clustering of momentary potential topographies into four microstate classes (A-D).
Results: In patients, microstates were shortened in classes B and D (from 80 to 70 ms, and from 94 to 82 ms, respectively), occurred more frequently in classes A and C, and covered more time in A and less in B. Topography differed only in class B where LORETA tomography predominantly showed stronger left and anterior activity in patients. - Microstate concatenations (syntax) generally was disturbed in patients; specifically, the class sequence A→C→D→A predominated in controls, but was reversed in patients (A→D→C→A).
Conclusions: In schizophrenics, information processing in certain classes of mental operations might deviate because of precocious termination. The intermittent occurrence might account for Bleuler's "double bookkeeping". The disturbed microstate syntax opens a novel, physiological comparison of mental operations between patients and controls.

Key Words:
Human EEG microstates; EEG spatial analysis; microstate transition probabilities; state dependency.

1. Introduction

Schizophrenic psychopathology typically is not homogenous over time; from moment to moment, patients might display or not display pathology. Disordered thoughts, hallucinatory percepts or delusional interpretations may repeatedly be present and not present during the same interview; the patient's state can change within fractions of a second, and frequently includes normal, reality-adequate thoughts and behavior. In fact, the instability of psychopathology is an adjuvant in diagnostics that distinguishes schizophrenic conditions from intoxication or drug conditions. Diagnostic classification, and ratings of the patients' verbalizations or of other behavior accordingly reflect the observations obtained over some time, at least minutes.

Similarly, physiological brain activity is measured over extended times, typically covering at least many seconds (EEG spectral analysis and EEG dimensional complexity, Event-Related Potentials, fMRI) up to several minutes (PET). In such studies, stability of functional state is not explicitly assumed, but variance over the measurement epochs is not examined. The time averages of psychological, behavioral and physiological measures have described numerous, clear differences between patient groups and normals. The results of these studies - which applied very different measurements and paradigms - converge on the concept that the disturbance underlying schizophrenic mentation is a degraded functional organization (a degraded connectivity, cooperativity, coordination) between brain processes and brain regions (e.g., Galderisi et al., 1992; Koukkou et al., 1993; Friston, 1996; Saito et al., 1998; Andreasen et al., 1999; Buchsbaum et al., 1999; Tononi and Edelman, 2000; Winterer et al., 2000; Josin and Liddle, 2001; Koenig et al., 2001; Strelets et al., 2001; Ford et al., 2002; Gruzelier, 2002; Gruzelier et al., 2002; Kubicki et al., 2002; Lawrie et al., 2002; Winterer et al., 2003).

But, the approaches above with their limited time resolution cannot assess the basic structure of the functional aberrations in the patients. Interactions of a person with his/her environment obviously occur within fractions of seconds when acting on and responding to environmental information. Spontaneous mentation and behavior in normal individuals as well as in schizophrenic patients varies in this time range. The behavior of schizophrenic patients with their rapid changes between reality-oriented and reality-remote thoughts and associations is a point in case (Bleuler, 1911).

A holistic approach to temporal segmentation of brain electric activity considers that the whole brain, as any other system, can be said to be in one particular state at each moment in time, however complex the state might be (Ashby, 1952). The momentary, spatial configuration of the brain electric field reflects the momentary state: Different spatial configurations of the brain electric field, i.e. different landscapes or distributions of brain potentials must have been caused by activity of different, cerebral generator neurons. It is reasonable to assume that activity of different neural populations incorporates different brain functions; thus, different distributions of brain potentials are indicative of different global, functional states.

Ongoing, spontaneous EEG can be displayed as series of instantaneous scalp maps of potential distributions or potential landscapes (Lehmann, 1971) by constructing a map of the potential values for each time point using all electrodes instead of the traditional construction of a waveshape for each electrode using all time points. Examination of the series of such momentary maps revealed that the maps' landscapes change in a non-continuous manner. Accordingly, the map series can be parsed into temporal segments of quasi-stable map landscapes, into 'microstates'. These microstates can be observed in spontaneous EEG (below) as well as in Event-Related Potentials (see e.g. Lehmann and Skrandies, 1980; Brandeis and Lehmann, 1989; Michel et al., 2001; Skrandies 2002). In wakeful, eyes closed, resting EEG, microstates showed mean durations of around 100 milliseconds (Lehmann et al., 1987). Different types of mentation (classes of thought) were associated with microstates of different potential landscapes (Lehmann et al., 1998); microstates were therefore suggested to be putative 'atoms of thought', basic psychophysiological units of cognition and emotion. Successive microstates accordingly would incorporate the corresponding, successive current contents of the global workspace proposed by Baars (1997). Microstates in spontaneous EEG were studied during development (Koenig et al., 2002), during normal levels of vigilance (Cantero et al., 1999) and in disease conditions (e.g., Merrin et al., 1990; Dierks et al., 1997; Kinoshita et al., 1995; Strik et al., 1997; Ihl and Brinkmeyer, 1998; Koenig et al., 2003). Concatenation between microstates was studied in normals, yielding an asymmetric transition matrix (Wackermann et al., 1993); it was hypothesized that normal and abnormal mentation might employ different concatenations of microstates (Lehmann et al., 1998).

These observations of a discontinuous structure of spontaneous brain electric activity that is formally segmentable into microstates lead to the conclusion that the subjectively continuous "stream of consciousness" is composed of identifiable building blocks. In this conceptual framework, the observation of seemingly coexisting psychotic and normal mentation and behavior in the patients would be accounted for by frequent, intermittent, and repeated occurrences of microstates with deviant properties or deviant concatenations, thereby causing the failure of some and the success of other cognitive operations within very short time intervals.

In two studies on young, first-episode, medication-naïve, acute schizophrenics, microstates were found to be shorter than in healthy controls (Koukkou et al., 1994; Kinoshita et al., 1998), while a third study (Table 2 in Stevens et al., 1999) also reported shortened mean durations, but no significant overall effect. A sequential microstate segmentation approach was used in these studies (Lehmann et al., 1987; Strik and Lehmann, 1993). An alternate, global approach for microstate analysis (Pascual-Marqui et al., 1995) sorts all data into a finite number of microstate classes. Applying this latter, global microstate analysis approach, Strelets et al. (2003) reported shortened microstate duration in one of four microstate classes in chronic, positive symptomatology schizophrenics, and Koenig et al. (1999) also reported microstate shortening preferentially for one of four microstate classes in young, first-episode, medication-naive schizophrenic patients.

To follow up on these findings, we analyzed data from 27 young, acute, first-episode, medication-naive patients and their controls that became available in cooperation with three independent centers.

We tested the hypotheses that microstates in young, first-episode, medication-naïve, acute schizophrenic patients (a) are generally shortened, that (b) this shortening selectively affects specific microstate class(es), and that (c) the concatenation (syntax) of the microstate classes is altered in the patients.

2. Methods

2.1. Subjects

EEG recordings were collected from young, acute, first-episode patients presenting with productive schizophrenic symptomatology before initiation of medication, and from age- and gender-matched controls. All subjects were self-reported right-handers. Subjects with prior medication, a history of alcohol or drug abuse, head trauma, epilepsy or other disease that might involve or affect brain functions were excluded. The data were collected in three institutions (centers): Neuropsychiatry Dept., Kansai Medical University, Osaka, Japan; Psychiatry Dept., University of Naples SUN, Italy; and Lab. Clin. Psychophysiol., Psychiatry Dept., University Hospital Benjamin Franklin, Free University of Berlin, Germany. Eventually, after careful review of the patient histories and of the EEG recordings, data from 27 patients and their matched (27) controls were included, 9 (9) from Osaka, 6 (6) from Naples, and 12 (12) from Berlin. Mean age of the 27 patients was 23.9 (S.D.=5.4, range=17-32) years, of the 27 controls 24.4 (S.D.=4.5, range=17-32). There were 9 women and 18 men in both groups. Eighteen of the patients were diagnosed as paranoid type (295.30), seven as undifferentiated type (295.90), and 1 each as hebephrenic type (295.10) and catatonic type (295.20), using DSM III-R in Osaka, DSM IV in Naples, and ICD-9 in Berlin.

The Ethics committees of the involved institutions accepted the study. The concept was explained to the patients and the control subjects, and written informed consent was obtained (from the parents if the patient was under age).

2.2. Recording and data preparation

Electrodes were attached according to the 21 standard locations of the International 10-20 System: 19 locations were used in Osaka (Fpz and Oz omitted), 16 in Naples (additionally omitted: Fz, Cz, Pz) and all 21 locations in Berlin, and recorded against linked earlobes, in Osaka with 0.3-30 Hz bandpass and digitized at 128 samples/sec/channel (Brain Atlas, Bio-logic Systems, Mundelein, IL, USA), in Naples and Berlin with 0.3-70 Hz, digitized in Naples at 312 samples/sec/channel (HZI Research Center, Tarrytown, NY, USA) and in Berlin at 166.6 samples/sec/channel (Walter Graphtek, Lübeck, Germany). The subject was comfortably seated and instructed to relax, and then, to close the eyes. The EEG data during this resting condition, starting with the moment of eye closure were used for further processing.

Off-line, all data were converted in Zurich to a common file format and digitally band-passed (2-20 Hz). The Berlin and Naples data were downsampled to 128 samples/sec/channel for convenience of further processing (this filtering and downsampling is compatible with the Nyquist sampling theorem). All data were divided into epochs of 2 seconds each for the Osaka and Berlin data, and 1.641 seconds for the Naples data (corresponding to 512 of the original samples, because epoch-divisioning had been done prior to band-passing). All data epochs were carefully reviewed for artifacts (eye movements, body movements, muscle activity, technical artifacts). Epochs contaminated with artifacts were rejected. For each subject, the first 20 artifact-free epochs (25 for Naples) starting immediately after eye closure were accepted from the available eyes-closed recordings. On the average, 36.7 seconds (S.D.=7.4) artifact-free EEG data were available for each patient, and 38.5 seconds (S.D.=4.4) for each control subject.

Then, all epochs were recomputed to average reference (i.e., removing spatial DC potential offset), and transformed into sequences of maps of momentary distributions of scalp potentials, thereby resulting in >250,000 momentary maps.

2.3. Microstate analysis

For the microstate analysis (Lehmann et al., 1987), the global approach (Pascual-Marqui et al., 1995; Koenig et al., 1999) was applied that sorts the submitted, momentary maps into a small number of map-landscape defined classes (software EMMA by T.Ko., free at www.puk.unibe.ch/tk2/tk.htm), as follows:

Out of all momentary maps, the maps with an optimal signal-to-noise ratio were selected for further analysis. This was done by computing a curve of Global Field Power (Lehmann and Skrandies, 1980) for each of the >1000 multichannel data epochs (each of 2 s duration for Osaka and Berlin, 1.641 s for Naples), thereby producing a one-number-value of field strength for each time point, i.e., producing a single curve from the multichannel data for each data epoch. At all time points of local maximal values of this curve of Global Field Power, i.e., of optimally pronounced potential landscape (optimal signal to noise ratio), the momentary potential distribution maps were selected for further analysis (called 'original maps'; see also Fig. 1); a total of over 40,000 original maps was thus entered into microstate analysis.

Microstate analysis started with a bottom-up path (steps 1-4 below) for the construction of the microstate classes, separately for the two subject groups and the three centers. Then followed a top-down path (steps 5-7) to identify corresponding microstate classes in the centers and groups, and to label the original maps. For all computations, the spatial configuration of the potential distributions was used while disregarding their polarity (Lehmann et al., 1987). The steps were as follows:

2.3.1. Four model maps for each subject. For each subject, using modified k-means clustering with repeatedly and randomly selected original maps as seeds, all original maps were clustered into four classes of maps following earlier studies (Pascual-Marqui et al., 1995; Koenig et al., 1999, 2002, 2003; Strelets et al., 2003). The clustering criterion was Global Map Dissimilarity (Lehmann and Skrandies, 1980) between the original maps, disregarding map polarity. The four microstate classes accounted for a mean of 83.4% (S.D.: 6.0%) of the data variance across patients, and of 84.6% (S.D.: 4.6%) across controls. For each of the four map classes of each subject, an 'individual model map' was computed by averaging all member maps of the class after permutating the maps' polarities for minimal variance of the mean.

2.3.2. Four classes of model maps common across subjects. Separately for each center, and separately for controls and patients, 'group model maps' were computed from the individual model maps. This procedure used k-means clustering as in (*2.3.1.*), but instead of selected seeds examined all possible seeds, and was constrained to produce one-to-one assignments of the subject's individual model maps to the group model maps. Two sets of four group model maps (a set for patients and a set for controls) resulted for each center.

2.3.3. Four model maps common for both groups. From the group model maps, for each of the three centers separately, four 'center model maps' were generated by averaging the best-fit pairs of the patients' and the controls' group model maps; the assignment procedure was identical to (2.3.2.).

2.3.4. Averages across centers. In order to combine the center model maps across centers, corresponding electrode positions were needed; the Osaka maps had 19 positions; the 2 additional positions in the Berlin maps were omitted, and the three missing midline positions in the Naples maps were linearly interpolated using the nearest neighbors' positions. Then, applying the procedure in (*2.3.2.*), one set of 'grand mean model maps' (four maps) were computed from the three sets of center model maps (four maps each). These four grand mean model maps were very similar to the four maps reported by Koenig et al. (1999) and therefore were labeled correspondingly as 'microstate classes' 'A', 'B', 'C' and 'D'.

2.3.5. Class-labeling of the center model maps: The class-labeled, four grand mean model maps were used to identify the microstate classes across centers. Each of the four center model maps of each center was class-labeled by assigning it to the best-fitting grand mean model map, using minimal Global Map Dissimilarity between the grand mean model maps and the tested center model maps as criterion, and permutation of the assignment for minimal overall variance. Thereafter, the electrode schemes of the center model maps were reconstituted for each center.

Thus, the interpolation and omission of electrodes in *2.3.4* was needed only for the alignment of the center model maps across centers. The subsequent labeling of the group model maps (*2.3.6*), and the following steps of recognition and labeling of the microstates (2.3.7) was done for each center after re-constitution of the original electrode schemes. The interpolation and omission of electrodes based on center model maps would therefore affect each center's controls and patients in identical ways and would not introduce systematic group effects. Also, when the averages across centers (*2.3.4.*) and the class-labeling of the center model maps (*2.3.5.*) was done using only the 16 electrodes that were common to all centers, the outcome remained identical, indicative of robust results.

2.3.6. Class-labeling of the group model maps. For each center, the four class-labeled center model maps with their re-constituted, original electrode schemes then served as templates to assign the four group model maps of the controls and the four group model maps of the patients to the four classes, and thereby label them as A, B, C and D. For each center, the labeled, four group model maps of the controls had a high common variance with the corresponding group model maps of the patients: Osaka 86.3%, Naples 81.7%, Berlin 88.3% (85.4% on the average across the three centers).

The class-labeled group model maps (4 microstate classes, 2 groups) of each center were used for the final step of the analysis.

2.3.7. Recognizing and labeling the microstates. In this final step, the class-labeled group model maps served as templates to assign each original map of each subject to one of the four microstate classes, separately for groups and centers, using minimal Global Map Dissimilarity between the group model maps and the tested original map as criterion. Successive original maps that were recognized to belong to the same microstate class were joined into one microstate. Fig. 1 illustrates an example. In the data from the 54 subjects, a total of over 23000 microstates were recognized and entered into final analysis. Four parameters of all microstates were computed for each microstate class of each subject (see below).

2.4. Visualization of the microstate class maps

For visualization of the potential landscapes of the four microstate classes, 'average group model maps' (Fig. 2) were computed from the labeled group model maps across the three centers, separately for patients and for controls. Since an equal number of channels was needed for this computation, the truncated or extended group model maps with 19 positions were used. However, the microstate parameters (below) were computed from the maps in their center-specific configurations (21, 19 and 16 electrode positions, respectively).

2.5. Microstate parameters

From the microstates of each subject, the following four parameters were computed:

'Duration' of a microstate is the time epoch, in milliseconds, during which all successive, original maps were assigned to the same microstate class, starting (ending) at the midpoint in time between the last original map of the preceding microstate and the first original map of the following microstate. For

each subject, mean microstate duration for each microstate class (A, B, C, D) was computed and, in addition, mean duration of all microstates regardless of microstate class assignment (labeled 'all').

'Occurrence/s' is the number of occurrences of the microstates of a given class (and, of all microstates regardless of class assignment) per second, across all analysis epochs.

'Time coverage' is the mean time in milliseconds (referred to 100 milliseconds) that was covered across all analysis epochs by all microstates of a given class; this value can also be read as percentage of time of the entire analysis time.

Note that for an individual subject, each of the three parameters duration, occurrence/s, and time coverage can be derived from the other two, but that this is not true anymore for the averages over subjects.

'Global Field Power peaks/s' is the total number of original maps (=peaks of Global Field Power) of a given class divided by the total time (in seconds) covered by this class. 'Global Field Power peaks/s' was also computed disregarding class assignment ('all'). Because Global Field Power reflects the global strength of the brain field, there are two maximal values of the Global Field Power curve during a conventional EEG wave, at the negative and positive peak; thus, EEG wave frequency is effectively doubled in Global Field Power curves, as it is e.g. in rectified EEG tracings.

A 2-way, fixed effects ANCOVA (2 groups × 4 microstate classes as repeated measures, 3 centers as covariate) was done for each of the four parameters.

2.6. Transitions between microstate classes

The rules governing the concatenation of the microstates ('microstate syntax') were assessed as follows. For each subject, the number of transitions from each of the four classes to any other class was counted; these figures were normalized to fractions of all between-class transitions of the subject (called 'transition percentages'). Twelve such transition values were thus obtained for each subject.

If transitions from a preceding state into a next state occurred randomly, i.e., independent of the class of the preceding state, observed transition values would be proportional to the relative occurrence of the microstate classes. Under this null-hypothesis, the expected probability of transition from state X to state Y is

$$P^*_{X\to Y} = P_X P_Y / (1 - P_X) ,$$

where P_X (P_Y) is the relative occurrence of microstate X (Y), i.e. the number of occurrences divided by the total number of microstates observed. Differences between observed and expected transition counts were tested as follows: expected transition probabilities and actually observed transition percentages were computed for each subject, and averaged across subjects. The difference between mean expected probabilities $P^*_{X\to Y}$ and mean observed transition percentages $P_{X\to Y}$ was then assessed using the chi-square distance

$$\Sigma_{X,Y} (P_{X\to Y} - P^*_{X\to Y})^2 / P^*_{X\to Y} ,$$

where the sum is taken over all $4 \times 4 - 4 = 12$ pairs of microstates for which $X \neq Y$. The randomization test (permutation test) was used to test statistically the significance of that distance (Edgington, 1980; Manly, 1997): The labels "expected" and "observed" were randomly assigned to the subjects' sets of the 12 transition probabilities, and the chi-square distance between expected and observed mean transition probabilities was computed. This was repeated 5000 times and thus produced a data-driven estimate of the distribution of the distance between the mean of the expected and the mean of the observed transition probabilities assuming the null-hypothesis is true. The probability that the observed data is compatible with the null-hypothesis (p-value) is determined by the rank of the observed difference among the randomly obtained differences. This test yielded P=0.0002 for the controls and P=0.0016 for the patients, which allows to rule out the null-hypothesis in both groups; we thus conclude that there is a structure in the observed transition values that cannot be reduced to the occurrence frequencies of the microstates.

Asymmetries of transitions between pairs of microstate classes would reveal directional tendencies in the microstate syntax. To examine these, we define the 'directional predominance' of transitions between each of the six possible pairings of microstate classes as

$$d_{XY} = P_{X\to Y} - P_{Y\to X} ,$$

i.e., the difference of the transition percentage between two given classes (X and Y) in one direction minus the corresponding transition percentage in the opposite direction.

The observed, directional predominances for the transitions between the six possible pairs of microstate classes were compared between patients and controls, applying a 2-way ANCOVA (2 groups × 6 direction predominances as repeated measures, 3 centers as covariate).

2.7. Spatial configuration of microstate classes

2.7.1. Global differences between map landscapes. The potential landscapes of the group model maps of each microstate class were compared statistically between groups, using the program 'TANOVA' by R.D.P.-M. (free at www.unizh.ch/keyinst/NewLORETA/LORETA01.htm); the program employs Global Map Dissimilarity (Lehmann and Skrandies, 1980) as a global measure of the difference between the landscapes of two maps; TANOVA applies the randomization test (Edgington, 1980; Manly, 1997, see preceding paragraph) to establish the exact probability of the observed difference, following earlier studies of potential landscapes (Kondakor et al., 1995; Strik et al., 1998). If TANOVA revealed significant landscape differences of a microstate class between groups, two subsequent analyses assessed the differences:

2.7.2. Primary characteristics of landscape difference. The different landscape topographies were assessed by computing the location of the brain electric gravity center on the anterior-posterior and on the left-right axis of the head (Lehmann et al., 1998); differences between patients and controls were tested by *t*-tests.

2.7.3. Intracerebral distribution of differences in brain electric activity. Low resolution electromagnetic tomography (LORETA) images (Pascual-Marqui et al., 1994, Pascual-Marqui, 1999) were computed from the individual model maps of the microstate class for all patients and controls. The utilized LORETA version (free at www.unizh.ch/keyinst/NewLORETA/LORETA01.htm) computed the electric current density (referred to as "activity") in the cortical areas of the digitized brain atlas of the Montreal Neurological Institute (MNI) at ~7 mm resolution (2394 voxels). Voxel-by-voxel *t*-statistics was computed to identify the voxels with strongest effect.

3. Results

3.1. Differences between patients and controls

3.1.1. Microstate parameters. Fig. 2 illustrates the average group model maps of the four microstate classes, independently computed for the patients and for the controls. The pairing of the four group model maps of the controls and of the patients for each center (3×4 paired classes) resulted in 85.4% of the variance in common across the three centers.

The ANCOVA's of the four microstate parameters (Table 1) revealed a significant group effect for duration and a trend for occurrence/s. A significant interaction between subject group and microstate class emerged for occurrence/s and for Global Field Power peaks/s, and a trend for time coverage. Note that the parameter time coverage cannot be tested for group differences because there is always a total of 100%.

Table 2 reports means and S.D. across subjects of the microstate parameters duration, occurrence/s, time coverage and Global Field Power peaks/s for the four microstate classes, for patients and controls. The posthoc *t*-tests in Table 2 clarified the source of the group effects and group x class interactions, and are briefly reviewed in the following.

Duration: The microstates of the classes B and D had significantly shorter durations in patients than controls, both by ~15%, i.e. from 80.3 to 70.1 ms (P=0.0021), and from 93.9 to 81.9 ms (P=0.027), respectively. When disregarding microstate classes ('all' in Table 2), generally shorter microstate duration was found in patients, supporting our hypothesis (a) with a statistical trend (one-tailed P=0.067).

Occurrence/s: The microstates of the classes A and C occurred more often in patients than controls (P=0.039, P=0.079, respectively). Class A increased from 2.17/second in controls to 2.91/second in patients, while class C increased from 3.15 to 3.45/second. When disregarding microstate classes, generally increased microstate occurrence/s for patients was found (P=0.075).

Time Coverage: Microstates of class A covered more of total time (P<0.025) in patients (~23%) than in controls (~17%); on the contrary, class B microstates tended to cover less of total time (P=0.064) in patients (~18%) than controls (~22%).

Global Field Power peaks/s: The posthoc tests of the significant group × class interaction revealed higher frequency for class B microstates in patients, but only at P=0.16.

3.1.2. Directional predominance of transitions between microstate classes ("microstate syntax"). The comparison between patients and controls of the, directional predominances of the transitions in the six possible pairs of microstate classes in a 2-way ANCOVA (2 groups × 6 direction predominances as repeated measures, 3 centers as covariate) showed no main effects, but a significant interaction (group × direction predominance): after Greenhouse-Geisser correction F(2.95,153.5)=2.77, P=0.045. Posthoc tests clarified that the transitions between microstate classes A and C, and between A and D differed significantly in directional predominance between groups, at P=0.05 and P=0.005, respectively (line #13 in Table 3, and upper half of Fig. 3). While controls had a predominance of A→C and D→A transitions, C→A and A→D transitions predominated in the patients, i.e., the two subject groups showed reversed tendencies of concatenations between the microstate classes A and C and between the classes A and D (lower half of Fig. 3).

Further tests examined the predominating directions of transitions between the four microstate classes in patients and controls (lines #6 and #9 in Table 3) for statistically significant deviation from zero values (Table 3, lines #8 and #11). In the patients, the predominating direction A→D approached a statistical trend (P=0.108). In the controls, A→C (P=0.006) and D→A (P=0.022) showed clearly predominant directions, and C→D yielded P=0.106. These three concatenations in the controls form a cycle A→C→D→A (Fig. 3, lower left). Although the corresponding three concatenations in the patients included only one directional predominance at P=0.108 (A→D), all three directions in this concatenation cycle were reversed in the patients compared with those of the controls, i.e. they were A→D→C→A.

Following up on this observation, for each subject, the observed cases of the three possible quadruplets in the sequence (A→C→D→A, C→D→A→C, and D→A→C→D) and of the three possible quadruplets in the reversed sequence (A→D→C→A, D→C→A→D, and C→A→D→C) were counted, and expressed as percentage of all possible quadruplets in the given subject. For each subject, the difference between the quadruplet percentages in the two directions was computed; these differences between patients and controls differed significantly (unpaired t-test P=0.031, t=2.23, df(corrected) =44). This global difference reflected the opposing directional preferences in the cycle: In patients, the sequence A→D→C→A was more frequent than the reversed sequence (averages across subjects 3.47% +/- 1.77 S.D. *vs.* 2.76% +/- 1.77 S.D., respectively), whereas in controls, the sequence A→D→C→A was less frequent than the reversed sequence (averages across subjects 2.10% +/- 1.45 S.D. *vs.* 2.50% +/- 1.03 S.D., respectively).

3.1.3. Spatial configuration of microstate classes. The global similarity test TANOVA revealed that only the scalp map landscapes of the potential distributions of microstates of class B (Fig. 2) differed significantly between patients and controls (P=0.043), while classes A, C and D showed no differences. The primary characteristics of this landscape difference were reflected by a significant location difference of the brain electric gravity center, more anterior by 0.09 electrode distances and more left by 0.10 electrode distances in patients than controls (P=0.013 and P<0.0001, respectively). LORETA functional tomography images of class B microstate maps (Fig. 4) showed stronger activity in patients than controls widespread in the left hemisphere (some also right prefrontal), with the extreme value (single-voxel t-test t=-4.12) in left precentral gyrus (Brodmann Area 6) at the Talairach coordinates X=-58, Y=4, Z=14 (=MNI coordinates -59, 3, 15); weaker activity in patients than controls was less pronounced, and centered around the extreme value (single-voxel t-test t=2.27) in right inferior parietal lobule (Brodmann Area 40) at the Talairach coordinates X=46 , Y=-36, Z=41 (=MNI coordinates 46, -39, 43).

3.2. Differences between microstate classes

The four microstate parameters of duration, occurrence/s, time coverage and Global Field Power peaks/s showed significant class effects in ANCOVA (Table 1), at $p<0.0001$ and $p<0.002$, respectively. Testing each microstate parameter between classes revealed, in all cases, significant differences between classes A *vs.* C and A *vs.* D, and B *vs.* C and B *vs.* D, but no significant differences between A *vs.* B and between C *vs.* D (all 54 subjects). The mean values of the four microstate classes for duration, occurrence/s and time coverage (Table 2) demonstrated, for both groups, lower values for classes A and B on one side and higher values for classes C and D on the other. A reversed ranking was displayed by Global Field Power peaks/s, with classes A and B showing the higher frequencies and C and D the lower ones.

4. Discussion

The present results of generally shorter microstate durations in acute, medication-naïve, first-episode schizophrenic patients are consistent with several earlier reports (see Introduction). In addition, the utilized, deeper analysis that considered classes of microstates showed that this general shortening in patients was due to significantly shorter durations in only two of the four microstate classes, i.e. in classes B and D. As apparent compensation, class A and C microstates in patients showed increased occurrence/s while displaying normal durations; time coverage was increased in A, and decreased in B. These findings are in good agreement with those on similar patients by Koenig et al. (1999) who also analyzed the data into four microstate classes; their four class model maps were very similar to the present ones, and their results generally agreed very well with the present ones. The latter is evident in the result profiles in Fig. 5. In particular, the durations in the four microstate classes of patients and of controls were almost identical in the two studies; the eight values correlated significantly between studies (Pearson $r=+0.80$, $df=6$, $P<0.05$). We note here that the present four class model maps accounted for 83.4% of the data variance across patients and 84.6% across controls. We also note that the paired group model maps of our controls and patients corresponded well, showing 85.4% of the variance in common across the three centers. Our four class model maps as well as those of Koenig et al. (1999) were very similar to the four class model maps obtained in a large, normative study on nearly 500 subjects (Koenig et al., 2002).

Accepting the concept that classes of spontaneous microstates incorporate classes of mental operations as shown in Lehmann et al. (1998), the observed, selective time truncation of some microstates, i.e. of those of classes B and D, suggests the functional consequence that the patients suffer from precocious termination of information processing in certain classes of mental operations, and that this occurs repetitively and intermittently in the continual sequence of successive, global microstates so that on the average over time, there is a clear deviation from the norm. The shortening of certain microstates is generally in line with the concept of degraded cooperativity of neural assemblies or functional processes in the patients (see Introduction) since it is reasonable to assume that lessened cooperativity within a network results in shortened durations of coordinated activity. In patients comparable to ours, using sequential and band-wise analysis, Merrin et al. (1990) observed an increased variability of microstate topography in the EEG theta frequency band, in line with the concept of loosened organization. Since the present analysis employed clustering and full-band data, it cannot test that finding. Important in our results is the specification that the different classes of neural activity were not equally affected; this would account for the ability of the patients to deal with many aspects of surround conditions in a satisfying way.

Only two other studies on patients used the same microstate clustering analysis as the present one. A study of productive, but chronic schizophrenics (Strelets et al., 2003) found significantly decreased duration of microstates of their class #1 that was argued to correspond to our class B, thus agreeing with the present results. On the other hand, they found no increase of occurrence/s and no increase of time coverage of their class #3 microstates (our class A), in contrast to the present and Koenig et al.'s (1999) results on first episode, never-medicated patients. Contrary to all three studies on schizophrenics, in Alzheimer patients an increased occurrence/s of class B microstates was found with increasing dementia (Koenig et al. 2003).

Global Field Power peaks/s that reflect EEG wave frequency as an estimate of global activation showed no overall difference between our patients and controls. The significant interaction between groups and microstate classes yielded an increase of wave frequency in class B microstates for patients at a mere $P=0.16$. At any rate, increased activation would only concern class B, not D. Indeed, in regard

to the parameters duration, occurrence/s, time coverage and peaks/s, the microstate classes evidently fell into two pairs, A and B vs. C and D that differed on all four parameters between pairs but on none within pairs. Thus, the parameters did not differentiate classes whose microstate duration was affected in our patients from classes that were not affected.

In an additional analysis, the present paper examined a novel aspect of brain electric microstates in schizophrenia that has not yet been studied until now: the hypothesis that there might be changes in microstate syntax. Indeed, in patients, the transitions between microstates of different classes deviated significantly from those in controls, and this difference was not explained by the different occurrence frequencies of the microstates. The sequence of concatenations of microstate class D→A→C→D was reversed in the patients; and, whereas controls showed clear directional preferences in transitions between the class D, A and C microstates, patients did not. The disturbed syntax also agrees with the concept of a degraded organization (connectivity, cooperativity; see Introduction) and the paralleling concept of more noise (Callaway et al., 1970; Donchin et al., 1970; Winterer et al., 2000) in the brain processes of the patients. It is not evident why class B with its shortened microstates was not involved in these most pronounced syntax changes while the other shortened microstate class (D) was involved. However, this lack of communality is in line with the absence of other common characteristics between classes B and D as discussed above. This microstate syntax analysis is new; there are no results as yet available from other patient populations for comparison.

What processing functions might the different classes of microstates incorporate? In several event-related potential (ERP) studies, microstates were shown to incorporate specific functions of information processing (e.g., Brandeis and Lehmann, 1989; Brandeis et al., 1995; Koenig and Lehmann, 1996; Michel et al., 2001; Pizzagalli et al., 2000; Skrandies 2002). For spontaneous EEG, the presently available information on the functional significance of microstates is very limited, only offering suggestions. Class A might concern abstract operations, class B concrete ones, since spontaneous, abstract thoughts and visual imagery, respectively were associated with comparable microstate topographies (Lehmann et al., 1998). Drawing on information from ERP studies, the present topographies of classes C (and D) resemble event-related potential microstates that were found to incorporate higher (and lower) degrees of attention (Brandeis and Lehmann, 1989). Further work is needed to clarify the functional significances of microstates in spontaneous EEG, and the degree up to which such microstate analysis may identify the expectedly limited number of superclasses of human mentation as physiological entities.

It is well known that schizophrenics have scalp EEG power topographies that differ from controls (e.g., John et al., 1988; Galderisi et al., 1992; Pascual-Marqui et al., 1999; Wuebben and Winterer, 2001). In the present analysis, these topographic differences were concentrated in class B microstates, the class that showed significant differences of spatial distribution. This disagrees with the earlier study (Koenig et al., 1999) that reported spatial differences for class D, but agrees with the findings by Strelets et al. (2003). The tomographic LORETA imaging of the present microstate class B in patients predominantly showed increased cortical activity in the left hemisphere (extending to right prefrontal) that was maximal left precentral, and some decreased activity centered around right inferior parietal regions. Although the full band LORETA activity measures cannot indicate whether the activity is excitatory or inhibitory, the predominantly anterior left-hemispheric excess might be inhibitory activity, because EEG frequency-band wise LORETA imaging in comparable patients had shown increase for the delta band in these regions (Pascual-Marqui et al., 1999).

In sum, the present findings agree with the concept of deteriorated connectivity or deteriorated functional organization and of increased noise in brain processes as suggested as a functional principle underlying schizophrenic symptomatology. Our findings specify that this disorganization, on the level of identifiable steps of mentation, may be implemented as precocious termination and deviant concatenation of some classes of brainwork. The present study does not elucidate the reason for the deviations, but describes the deviating brain mechanisms with a time resolution that is well in the subsecond range and therefore appropriate for studies of physiological incorporation of mentation. The results could account for the fact that some of the patients' mentations are deviant, and that others are not. The intermittent, repetitive and brief nature of the microstate abnormalities in the patients fits well with the instantaneous switches in observable symptomatology, and could account for the ability to alternate smoothly between normal involvement in the surround and various reality-remote interpretations and delusions, the classical "double bookkeeping" (Bleuler, 1911) of schizophrenic patients; the latter might

be implemented by a "time-sharing"-type access of intermittent, deviant microstates to conscious experience.

Acknowledgments

This work was supported in part by grant #670806 to D.L. from the Institut für Grenzgebiete der Psychologie und Psychohygiene, Freiburg i.B., and by grant #Wi1316/2-1 to G.W. from the Deutsche Forschungsgemeinschaft. We thank Dr. L.R.R. Gianotti for critical comments.

References

Andreasen, N.C., Nopoulos, P., O'Leary, D.S., Miller, D.D., Wassink, T., Flaum, M., 1999. Defining the phenotype of schizophrenia: cognitive dysmetria and its neural mechanisms. Biological Psychiatry 46, 908-920.

Ashby, W.R., 1952. Design for a Brain. Wiley, New York.

Baars, B.J., 1997. In the Theater of Consciousness : the Workspace of the Mind. Oxford University Press: New York.

Bleuler, E., 1911. Dementia Praecox oder Gruppe der Schizophrenien. Deuticke, Leipzig.

Brandeis, D., Lehmann, D., 1989. Segments of ERP map series reveal landscape changes with visual attention and subjective contours. Electroencephalography and Clinical Neurophysiology 73, 507-519.

Brandeis, D., Lehmann, D., Michel, C.M., Mingrone, W., 1995. Mapping event-related potential microstates to sentence endings. Brain Topography 8, 145-159.

Buchsbaum, M.S., Hazlett, E.A., Haznedar, M.M., Spiegel-Cohen, J., Wei, T.C., 1999. Visualizing fronto-striatal circuitry and neuroleptic effects in schizophrenia. Acta Psychiatrica Scandinavica Supplement 395, 129-137.

Callaway, E. 3rd, Jones, R.T., Donchin, E. 1970. Auditory evoked potential variability in schizophrenia. Electroencephalography and Clinical Neurophysiology 29, 421-428.

Cantero, J.L., Atienza, M., Salas, R.M., Gomez, C.M., 1999. Brain spatial microstates of human spontaneous alpha activity in relaxed wakefulness. Brain Topography 11, 257-263.

Dierks, T., Jelic, V., Julin, P., Maurer, K., Wahlund, L.O., Almkvist, O., Strik, W.K., Winblad, B., 1997. EEG-microstates in mild memory impairment and Alzheimer's disease: Possible association with disturbed information processing. Journal of Neural Transmission 104, 483–495.

Donchin, E., Callaway, E. 3rd, Jones, R.T., 1970. Auditory evoked potential variability in schizophrenia. II. The application of discriminant analysis. Electroencephalography and Clinical Neurophysiology 29, 429-440.

Edgington, E.S., 1980. Randomization Tests. Dekker, New York.

Ford, J.M., Mathalon, D.H., Whitfield, S., Faustman, W.O., Roth, W.T., 2002. Reduced communication between frontal and temporal lobes during talking in schizophrenia. Biological Psychiatry 51, 485-492.

Friston, K.J., 1996. Theoretical neurobiology and schizophrenia. British Medical Bulletin 52, 644-655.

Galderisi, S., Mucci, A., Mignone, M.L., Maj, M., Kemali, D., 1992. CEEG mapping in drug-free schizophrenics: differences from healthy subjects and changes induced by haloperidol treatment. Schizophrenia Research 6, 15-24.

Gruzelier, J., 2002. A Janusian perspective on the nature, development and structure of schizophrenia and schizotypy. Schizophrenia Research 54, 95-103.

Gruzelier, J., Galderisi, S., Strik, W., 2002. Neurophysiological research in psychiatry. In: Lopez-Ibor, J.J., Gaebel, W., Maj, M., Sartorius, N. (Eds.), Psychiatry as a Neuroscience. Wiley, New York, pp. 125-180.

Ihl, R., Brinkmeyer, J., 1998. Differential diagnosis of aging, dementia of the Alzheimer type and depression with EEG segmentation. Dementia and Geriatric Cognitive Disorders 10: 64-69.

John, E.R., Prichep, L.S., Fridman, J., Easton, P., 1988. Neurometrics: computer-assisted differential diagnosis of brain dysfunctions. Science 239, 162-169.

Josin, G.M., Liddle, P.F., 2001. Neural network analysis of the pattern of functional connectivity between cerebral areas in schizophrenia. Biological Cybernetics 84, 117-122.

Kinoshita, T., Kuginuki, T., Yagyu, T., Saito, N., Hirota, T., Saito, M., 1998. Spatial EEG field configuration in schizophrenics. Psychiatry Research Neuroimaging 83, 58.

Kinoshita, T., Strik, W.K., Michel, C.M., Yagyu, T., Saito, M., Lehmann, D., 1995. Microstate segmentation of spontaneous multichannel EEG map series under diazepam and sulpiride. Pharmacopsychiatry 28: 51-55.

Koenig, T., Lehmann, D., 1996. Microstates in language-related brain potential maps show noun-verb differences. Brain and Language 53, 169-182.

Koenig, T., Lehmann, D., Merlo, M., Kochi, K., Hell, D., Koukkou, M., 1999. A deviant EEG brain microstate in acute, neuroleptic-naïve schizophrenics at rest. European Archives of Psychiatry and Clinical Neuroscience 249, 205-211.

Koenig, T., Lehmann, D., Saito, N., Kuginuki, T., Kinoshita, T., Koukkou, M., 2001. Decreased functional connectivity of EEG theta frequency activity in first-episode, neuroleptic-naïve patients with schizophrenia: preliminary results. Schizophrenia Research 50, 55-60.

Koenig, T., Prichep, L., Lehmann, D., Sosa, P.V., Braeker, E., Kleinlogel, H., Isenhart, R., John, E.R., 2002. Millisecond by millisecond, year by year: normative EEG microstates and developmental stages. NeuroImage 16, 41-48.

Koenig, T., Jelic, V., Hubl, D., Wahlund, L.O., Dierks, T., John, E.R., Prichep, L., 2003. EEG Spatiotemporal Dynamics in Alzheimer's Disease. Brain Topography 15, 193.

Kondakor, I., Pascual-Marqui, R.D., Michel, C.M., Lehmann, D., 1995. Event-related potential map differences depend on the pre-stimulus microstates. Journal of Medical Engineering and Technology 19, 66-69.

Koukkou, M., Lehmann, D., Strik, W.K., Merlo, M.C., 1994. Maps of microstates of spontaneous EEG in never-treated acute schizophrenia. Brain Topography 6, 251-252.

Koukkou, M., Lehmann, D., Wackermann, J., Dvorak, I., Henggeler, B., 1993. Dimensional complexity of EEG brain mechanisms in untreated schizophrenia. Biological Psychiatry 33, 397-407.

Kubicki, M., Westin, C.F., Maier, S.E., Frumin, M., Nestor, P.G., Salisbury, D.F., Kikinis, R., Jolesz, F.A., McCarley, R.W., Shenton, M.E., 2002. Uncinate fasciculus findings in schizophrenia: a magnetic resonance diffusion tensor imaging study. American Journal of Psychiatry 159, 813-820.

Lawrie, S.M., Buechel, C., Whalley, H.C., Frith, C.D., Friston, K.J., Johnstone, E.C., 2002. Reduced frontotemporal functional connectivity in schizophrenia associated with auditory hallucinations. Biological Psychiatry 51, 1008-1011.

Lehmann, D., 1971. Multichannel topography of human alpha EEG fields. Electroencephalography and Clinical Neurophysiology 31, 439-449.

Lehmann, D., Skrandies, W., 1980. Reference-free identification of components of checkerboard-evoked multichannel potential fields. Electroencephalography and Clinical Neurophysiology 48, 609-621.

Lehmann, D., Ozaki, H., Pal, I., 1987. EEG alpha map series: brain micro-states by space-oriented adaptive segmentation. Electroencephalography and Clinical Neurophysiology 67, 271-288.

Lehmann. D., Strik, W.K., Henggeler, B., Koenig, T., Koukkou, M., 1998. Brain electric microstates and momentary conscious mind states as building blocks of spontaneous thinking: I. Visual imagery and abstract thoughts. International Journal of Psychophysiology 29, 1-11.

Manly, B.F.J., 1997. Randomization, Bootstrap and Monte Carlo Methods in Biology. Chapman and Hall, London.

Merrin, E.L., Meek, P., Floyd, T.C., Callaway, E. 3rd., 1990. Topographic segmentation of waking EEG in medication-free schizophrenic patients. International Journal of Psychophysiology 9, 231-236.

Michel, C.M., Thut, G., Morand, S., Khateb, A., Pegna, A.J., Grave de Peralta, R., Gonzales, S., Seeck, M., Landis, T., 2001. Electric source imaging of human brain functions. Brain Research Reviews 36, 108-118.

Pascual-Marqui, R.D., 1999. Review of methods for solving the EEG inverse problem. International Journal of Bioelectromagnetism 1, 75-86.

Pascal-Marqui, R.D., Michel, C.M., Lehmann, D., 1994. Low resolution electromagnetic tomography: a new method for localizing electrical activity in the brain. International Journal of Psychophysiology 18, 49-65.

Pascual-Marqui, R.D., Michel, C.M., Lehmann, D., 1995. Segmentation of brain electrical activity into microstates: model estimation and validation. IEEE Transactions of Biomedical Engineering 42, 658-665.

Pascual-Marqui, R.D., Lehmann, D., Koenig, T., Kochi, K., Merlo, M.C.G., Hell, D., Koukkou, M., 1999. Low resolution brain electromagnetic tomography (LORETA) functional imaging in acute, neuroleptic-naive, first-episode, productive schizophrenics. Psychiatry Research Neuroimaging 90, 169-179.

Pizzagalli, D., Lehmann, D., Koenig, T., Regard, M., Pascual-Marqui, R.D., 2000. Face-elicited ERPs and affective attitude: brain electric microstate and tomography analyses. Clinical Neurophysiology 11, 521–531.

Saito, N., Kuginuki, T., Yagyu, T., Kinoshita, T., Koenig, T., Pascual-Marqui, R.D., Kochi, K., Wackermann, J., Lehmann, D., 1998. Global, regional and local measures of complexity of multichannel EEG in acute, neuroleptic-naive, first-break schizophrenics. Biological Psychiatry 43, 794-802.

Skrandies, W., 2002. Electroencephalogram (EEG) Topography. In: Hornak, J. P. (Ed.), The Encyclopedia of Imaging Science and Technology, Vol. 1. Wiley, New York, pp. 198-210.

Stevens, A., Mattes, R., Günther, W., Müller, N., Trapp, W., 1999. First episode schizophrenics show normal duration and topography of quasistationary EEG segments as compared to controls, during rest as well as during active tasks. Psychiatry Research Neuroimaging 91, 111-120.

Strelets, V.B., Novototski-Vlasov, V.I., Golikova, Zh.V., 2001. [Cortical connectivity in schizophrenic patients with positive and negative symptoms] [Russian] Zhurnal vysshei nervnoi deiatelnosti imeni I P Pavlova 51, 452-460.

Strelets, V., Faber, P.L., Golikova, J., Novototsky-Vlasov, V., Koenig, T., Gianotti, L.R.R., Gruzelier, J.H., Lehmann, D., 2003. Chronic schizophrenics with positive symptomatology have shortened EEG microstate durations. Clinical Neurophysiology 14, 2043-2051.

Strik, W.K., Chiaramonti, R., Muscas, G.C., Paganini, M., Mueller, T.J., Fallgatter, A.J., Versari, A., Zappoli, R., 1997. Decreased EEG microstate duration and anteriorisation of the brain electrical fields in mild and moderate dementia of the Alzheimer type. Psychiatry Research 75, 183–191.

Strik, W.K., Lehmann, D., 1993. Data-determined window size and space-oriented segmentation of spontaneous EEG map series. Electroencephalography and Clinical Neurophysiology 87, 169-174.

Strik, W.K., Fallgatter, A.J., Brandeis, D., Pascual-Marqui, R.D., 1998. Three-dimensional tomography of event-related potentials during response inhibition: evidence for phasic frontal lobe activation. Electroencephalography and Clinical Neurophysiology 108, 406-413.

Tononi, G., Edelman, G.M., 2000. Schizophrenia and the mechanisms of conscious integration. Brain Research Brain Research Reviews 31, 391-400.

Wackermann, J., Lehmann, D., Michel, C.M., Strik, W.K., 1993. Adaptive segmentation of spontaneous EEG map series into spatially defined microstates. International Journal of Psychophysiology 14, 269-283.

Winterer, G., Coppola, R., Egan, M.F., Goldberg, T.E., Weinberger, D.R., 2003. Functional and effective frontotemporal connectivity and genetic risk for schizophrenia. Biological Psychiatry 54, 1181-1192.

Winterer, G., Ziller, M., Dorn, H., Frick, K., Mulert, C., Wuebben, Y., Herrmann, W.M., Coppola, R., 2000. Schizophrenia: reduced signal-to-noise ratio and impaired phase-locking during information processing. Clinical Neurophysiology 111, 837-849.

Wuebben, Y., Winterer, G., 2001. Hypofrontality -- a risk-marker related to schizophrenia? Schizophrenia Research 48, 207-217.

Table 1

Results of the 2-way ANCOVA's (2 subject groups × 4 microstate classes as repeated measure, 3 centers as covariate) for the four microstate parameters, with Greenhouse-Geisser corrections where needed. N/A = computation for group effect of 'time coverage' is not applicable because total coverage is always 100% time. Data from 27 patients vs. 27 controls.

	df	*F*	*p*
duration (ms)			
group	1, 51	6.39	0.015
class	2.37, 123	10.86	<0.0001
interaction	2.37, 123	1.29	n.s.
occurrence / s			
group	1, 51	3.31	0.075
class	2.39, 124	17.39	<0.0001
interaction	2.39, 124	4.02	0.015
time coverage (ms/100ms)			
group	N/A	N/A	N/A
class	2.40, 125	15.22	<0.0001
interaction	2.40, 125	2.33	0.091
Global Field Power peaks / s			
group	1, 51	0.06	n.s.
class	1.82, 94.6	7.21	0.0017
interaction	1.82, 94.6	3.29	0.046

Table 2

Results of the microstate analysis. Means and standard deviations (patients *n*=27, controls *n*=27), of the four microstate parameters for the four microstate classes, and when disregarding class assignment ("all" microstates). Two-tailed *P*-values <0.1 of differences between patients and controls are reported. *) = one-tailed *P*, testing the literature-based hypothesis (a) that there is a generally shortened duration. N/A=because total coverage of time is always 100%, there is no applicable mean coverage when disregarding class assignment. **) = the tabulated values of Global Field Power peaks/s for "all" microstates are the mean values for the entire analysis time.

microstate classes	A	B	C	D	all
duration (ms)					
patients mean	76.7	70.1	89.6	81.9	84.5
S.D.	20.0	12.5	26.1	17.8	13.7
controls mean	75.6	80.3	95.0	93.9	89.9
S.D.	14.6	10.4	23.0	22.0	12.0
P	-	0.0021	-	0.027	0.067*)
occurrence / s					
patients mean	2.91	2.47	3.45	3.29	12.12
S.D.	1.12	0.90	0.53	0.74	1.85
controls mean	2.17	2.68	3.15	3.30	11.30
S.D.	0.66	0.78	0.68	0.60	1.38
P	0.039	-	0.079	-	0.075
time coverage (ms/100ms)					
patients mean	22.9	17.8	31.7	27.5	100.0
S.D.	12.5	7.4	13.0	9.8	-
controls mean	16.7	21.5	30.4	31.3	100.0
S.D.	7.1	6.9	10.8	10.0	-
P	0.025	0.064	-	-	N/A
Global Field Power peaks / s					
patients mean	20.2	20.8	19.8	20.0	20.2 **)
S.D.	1.22	2.01	0.94	0.95	1.07
controls mean	20.4	20.2	20.0	19.9	20.1 **)
S.D.	1.16	1.09	1.28	1.25	1.14
P	-	0.16	-	-	-

Table 3

A. Mean of percentages of all transitions between microstate classes/subject, for patients (*n*=27) and controls (*n*=27). - B. Directional predominances for the possible six pairs of corresponding transitions, in patients and controls; ANCOVA (2 groups × 6 directional predominances, 3 centers as covariate) interaction (Greenhouse-Geisser corrected) $F(2.95,153.5)=2.77$, $P=0.045$. Mean differences between patients and controls in line #12, significances of these differences line #13. Lines #8 and #11 show significances of deviation of mean values from zero. Differences (lines #5 and #12) are values of patients minus controls. *P*-values <0.2 are listed.

A. Transition Percentages

from class ® to class

		A ® B	**B ® A**	**A ® C**	**C ® A**	**A ® D**	**D ® A**	**B ® C**	**C ® B**	**B ® D**	**D ® B**	**C ® D**	**D ® C**
	patients												
#1	mean	6.47	6.73	9.20	9.37	7.83	7.44	6.65	6.56	6.56	6.84	13.16	13.21
#2	(S.D.)	(3.15)	(3.24)	(3.57)	(4.43)	(2.90)	(2.72)	(3.08)	(3.30)	(2.69)	(2.88)	(8.73)	(8.52)
	controls												
#3	mean	5.70	5.73	7.52	6.81	6.03	6.70	7.71	7.87	9.99	9.86	13.23	12.80
#4	(S.D.)	(2.35)	(2.63)	(3.05)	(3.43)	(2.34)	(2.24)	(3.04)	(2.74)	(4.23)	(3.75)	(5.54)	(5.31)
#5	difference	0.77	1.00	1.67	2.55	1.80	0.74	-1.07	-1.31	-3.43	-3.03	0.07	-0.41

B. Directional Predominances

		A ® B minus **B ® A**	**A ® C** minus **C ® A**	**A ® D** minus **D ® A**	**B ® C** minus **C ® B**	**B ® D** minus **D ® B**	**C ® D** minus **D ® C**
	patients						
#6	mean	-0.26	-0.17	0.39	0.09	-0.27	-0.05
#7	(S.D.)	(1.42)	(1.96)	(1.20)	(1.49)	(1.11)	(1.51)
#8	*t*-test *P* mean *vs. zero*	-	-	**0.108**	-	-	-
	controls						
#9	Mean	-0.03	0.71	-0.67	-0.16	0.13	0.43
#10	(S.D.)	(1.28)	(1.22)	(1.44)	(1.41)	(1.49)	(1.34)
#11	*t*-test *P* mean *vs. zero*	-	**0.006**	**0.022**	-	-	**0.106**
#12	difference patients minus controls	-0.23	-0.88	1.06	0.25	-0.40	-0.48
#13	*t*-test *P* for patients *vs.*controls	-	**0.05**	**0.005**	-	-	-

Legends for the Figures

Fig. 1. Example of the assignment of 'original maps' (dots along the horizontal axis) at the times of maximal Global Field Power (curve at bottom) to the four group model maps, i.e., microstate classes. Each original map is assigned to the group model map with the most similar potential landscape. The illustrated isopotential contour maps show the areas of opposite polarity in black and white. Note that the spatial distribution of the potential values is the crucial parameter in microstate analysis of spontaneous EEG; polarity is disregarded.

Fig. 2. The group model maps (average across centers) of the four microstate classes, independently computed for the controls (n=27) and the patients (n=27). Equipotential area maps are shown, normalized across subjects in order to compare the characteristics of the potential landscapes. Semi-schematic electrode array in inset. Head seen from above, nose up, left ear left. The isopotential contour maps show the (arbitrarily assigned) areas of opposite polarity in black and white (normalized voltage values).

Fig. 3. Syntax of microstate concatenations in patients and controls. Upper graphs, left: schematic arrangement of the four microstate classes A, B, C, D and the six possible transitions between them; right: Transitions between A and C (P=0.05) and between A and D (P=0.005) showed significant differences in directional predominance between patients and controls. Lower graphs: Directional predominance of transitions differed from zero at P<0.2 (solid arrows) in controls for A→C (P=0.006), C→D (P=0.106) and D→A (P=0.022), and in patients for A→D (P=0.108).

Fig. 4. LORETA (low resolution electromagnetic tomography) brain images of the statistical difference in cortical distribution of electric sources of class B microstates between patients and controls. Left to right: slices in axial (from above, nose up), sagittal (from left) and coronal (from rear) view in MNI space. Blue= stronger activity in patients, red= stronger activity in controls. The post-hoc t-test results are color-coded from deep blue for extreme negative, to white for zero, to deep red for extreme positive t-values. Upper row: slices through the voxel (indicated by arrowheads) of maximally stronger activity in patients (t=-4.12). Lower row: slices through the voxel (indicated by arrowheads) of maximally stronger activity in controls (t=2.27). The MNI coordinates (X, Y, Z) of these voxels are reported in mm.

Fig. 5. Comparison of the results of the microstate parameters of duration, occurrence/s, and covered time for the four microstate classes A-D in the present study and in Koenig et al. (1999) that used the same analysis strategy on comparable patients. Results are shown if P<0.2 was reached in either study. Slashes (/) or backslashes (\) indicate that patients had larger or smaller values than controls, respectively. /,\ = P>0.2; //,\\ = P=0.2-0.1; ///,\\\ = P=0.1-0.05; ////,\\\\ = P<0.05.

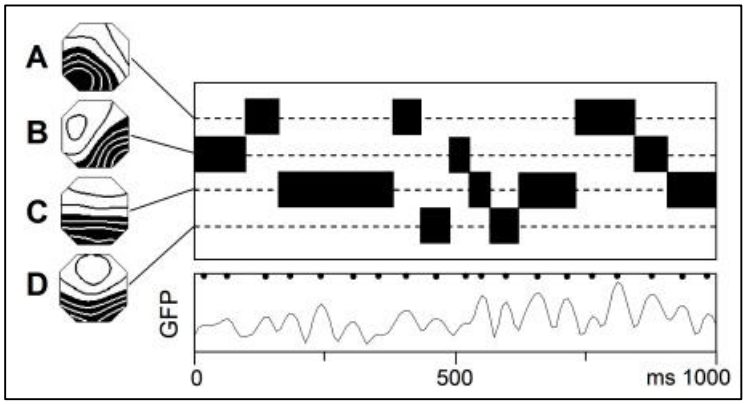

Fig. 1

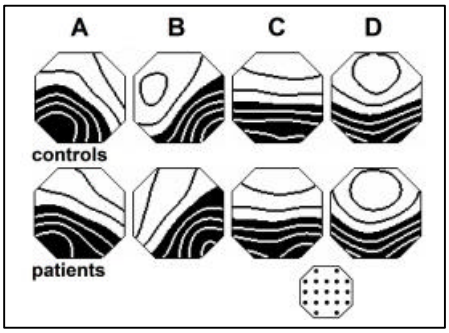

Fig. 2

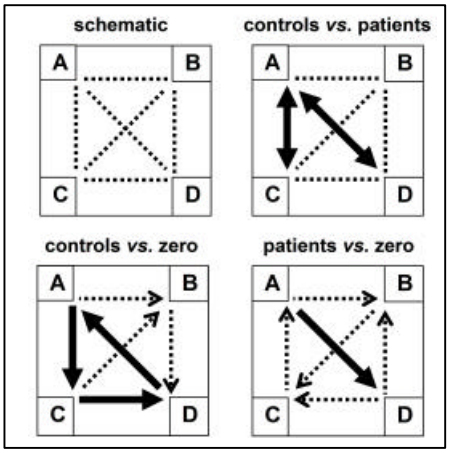

Fig. 3

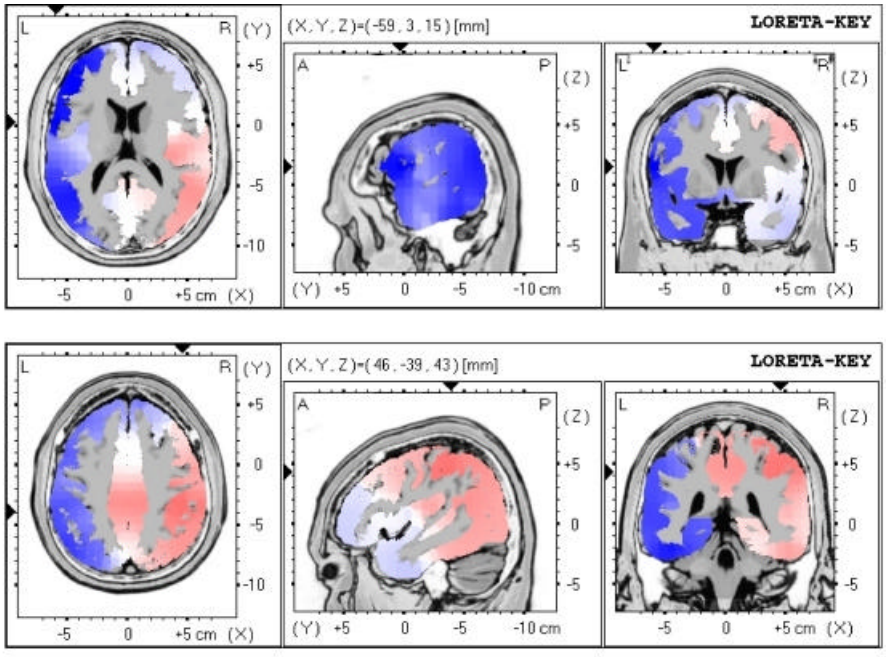

Fig. 4

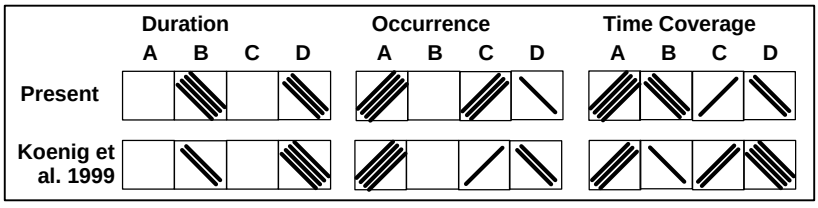

Fig. 5